Atomic-Scale Mechanical Properties of Orientated C-60 Molecules Revealed by Noncontact Atomic Force Microscopy

ARTICLE *in* ACS NANO · AUGUST 2011

Impact Factor: 12.88 · DOI: 10.1021/nn201462g · Source: PubMed

5 AUTHORS, INCLUDING:

Rémy Pawlak
University of Basel
34 PUBLICATIONS **430** CITATIONS
SEE PROFILE

Shigeki Kawai
University of Basel
80 PUBLICATIONS **784** CITATIONS
SEE PROFILE

Thilo Glatzel
University of Basel
133 PUBLICATIONS **2,520** CITATIONS
SEE PROFILE

Ernst Meyer
University of Basel
362 PUBLICATIONS **12,446** CITATIONS
SEE PROFILE

Atomic-Scale Mechanical Properties of Orientated C_{60} Molecules Revealed by Noncontact Atomic Force Microscopy

Rémy Pawlak,* Shigeki Kawai, Sweetlana Fremy, Thilo Glatzel, and Ernst Meyer

Department of Physics, University of Basel, Klingbergstrasse 82, 4056 Basel, Switzerland

ABSTRACT In this work, the mechanical properties of C_{60} molecules adsorbed on Cu(111) are measured by tuning-fork-based noncontact atomic force microscopy (nc-AFM) and spectroscopy at cryogenic conditions. Site-specific tip–sample force variations are detected above the buckyball structure. Moreover, high-resolution images obtained by nc-AFM show the chemical structure of this molecule and describes unambiguously its orientations on the surface.

KEYWORDS: noncontact atomic force microscopy · scanning tunnelling microscopy · three-dimensional dynamic force spectroscopy · fullerene C_{60} · high-resolution imaging · local force variation

Ever since its discovery in 1985 by Kroto *et al.*,[1] fullerene has always attracted a considerable interest toward single-molecular devices.[2–5] Although the orientation of C_{60} adsorbed between metallic electrodes plays a crucial role in its electronic property,[6,7] no straightforward approach to resolve directly its orientation has been established yet. High-resolution scanning tunnelling microscopy (STM)[8] imaging opened up a field to study individual molecules adsorbed on conductive surfaces and has significantly increased the understanding of their self-assemblies[9] and their reactivities.[10,11] However, since STM probes the local electronic density of states near the Fermi level and molecular orbitals are usually extended over the entire molecule, atomic features within a molecule are usually obscured. Although numerous attempts have been performed by STM to corroborate the complex molecular orbital patterns of C_{60}, theoretical calculations were always required for understanding their orientations on the surface.[12–15]

Since the first systematic achievement of atomic resolution in 1995,[16] noncontact atomic force microscopy (nc-AFM) became an important tool for real-space high-resolution imaging.[17] The tip–sample interaction force gradient is detected *via* the resonance frequency shift Δf of the oscillating cantilever. The atomic resolution mainly arises from the short-range interaction while the long-range force does not give specific information. In contrast to STM, the local electronic density of states surrounding a molecule has a relatively weak impact on the force field probed by nc-AFM. Advances in this technique[18] have recently demonstrated the resolution of the inner structure within adsorbed molecules such as pentacene and perylene-3,4,9,10-tetracarboxylic-3,4,9,10-dianhydride (PTCDA) *via* the detection of the repulsive tip–sample interaction with a CO-terminated tip.[19–21] Since the intrinsic properties of the sample, such as flatness, stiffness, mobility, and reactivity, are always crucial for stable imaging conditions, pure carbon materials such as graphite are known as one of the most difficult samples for nc-AFM imaging.[22–25] Indeed, in these van der Waals (vdW) surfaces the site-dependent interaction forces arising between tip and carbon atoms induce smooth potential corrugations.[24,26] Moreover, atomically resolved images on three-dimensional carbon objects like nanotubes are also problematic since the flatness is locally lost.[27,28] For these reasons, C_{60} would be the most challenging sample for such atomic-scale investigations. So far, nc-AFM investigations of C_{60} have been essentially focused on the growth properties of self-assemblies.[29–31]

In this paper, the chemical structure of C_{60} molecules adsorbed on Cu(111) is resolved by nc-AFM which gives a direct and unambiguous observation of their orientations on the surface. Systematic three-dimensional force spectroscopic measurements performed above single C_{60} molecules reveal that Pauli repulsive forces are required to reach such intramolecular resolutions. The detection of site-dependent tip–sample force variations above the buckyball structure is demonstrated at the atomic scale.

* Address correspondence to remy.pawlak@unibas.ch.

Received for review April 20, 2011 and accepted July 7, 2011.

Published online July 07, 2011
10.1021/nn201462g

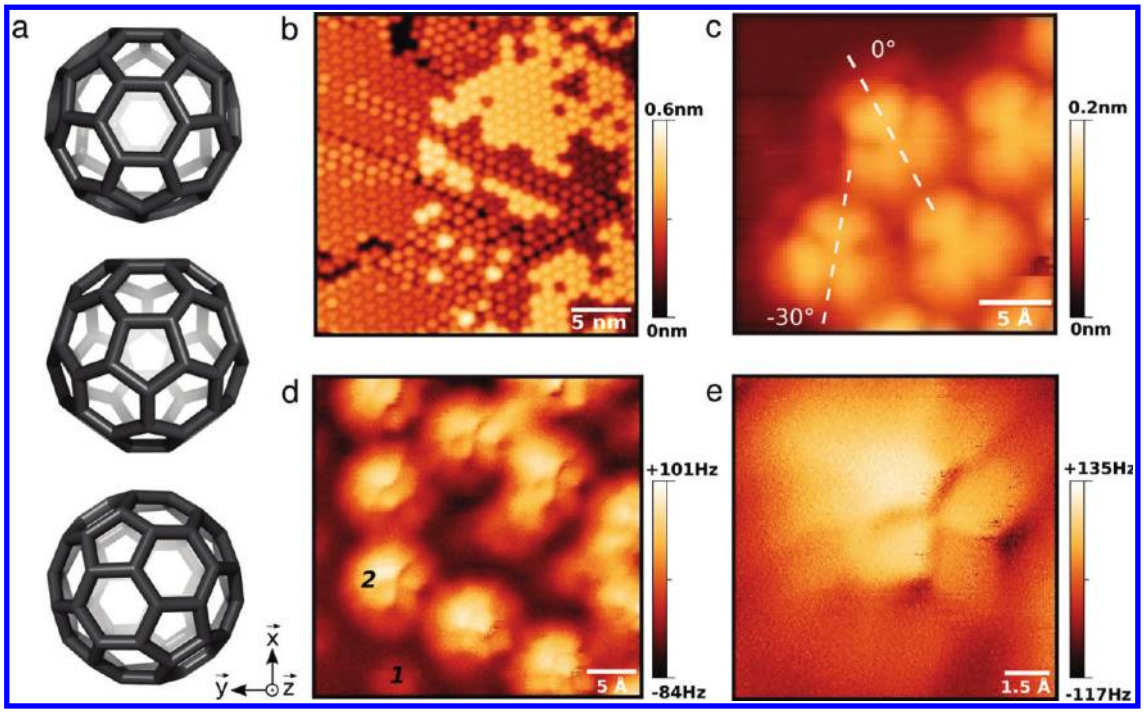

Figure 1. (a) Scheme of different possible orientations of the C_{60} molecule. (b) Constant-current STM image performed at $T = 77$ K on top of a C_{60} island grown on Cu(111) revealing different molecular orbitals ($I_t = 200$ pA, $V_t = -1.9$ V, no tuning fork oscillation). Panel c shows a more detailed STM image where all molecules have the same vertical orientation but different azimuthal angles (marked in the image) ($I_t = 50$ pA, $V_t = -500$ mV, resonant oscillation $A = 40$ pm). (d) Constant-height nc-AFM image recorded at 5 K above two layers of self-assembled C_{60} molecules, marked 1 and 2, showing directly the C_{60} atomic structures of the layer 2, ($A = 50$ pm, $V_t = 0$ V). (e) High-resolution image of a C_{60} molecule recorded with nc-AFM at constant height ($A = 60$ pm, $V_t = 0$ V).

RESULTS AND DISCUSSION

STM and nc-AFM experiments were performed with a tuning-fork-based STM/nc-AFM microscope running at low temperature (77 and 5 K) in an ultrahigh vacuum chamber. All STM images were recorded at constant current mode with the bias voltage applied to the tip, and the nc-AFM images were acquired at constant height or at constant current (see Supporting Informations Figures S1 and S2). The C_{60} molecules were deposited from an effusion cell (650 K, 1 min) onto the atomically cleaned Cu(111) surface kept at room temperature resulting in a coverage of approximatively 50−60% of a monolayer.

For this coverage, C_{60} exhibits an island growth mode on Cu(111) and the molecule adsorbs with several different orientations[14] depicted schematically in Figure 1a. Since three independent parameters, the binding site of C_{60} to the surface (polar angle), the surface site and the rotation of the C_{60} (azimuthal angle) modifies the charge transfer trough the molecule,[14] a large set of contrasts is usually detected by STM[12] as shown Figure 1b. Figure 1c shows a STM topography of C_{60} of the second molecular layer, measured at a negative tip bias voltage (−500 mV). The 3-fold symmetry pattern is typical for the lowest unoccupied molecular orbitals with a pentagon facing the tip,[6,14] and the rotation of the observed contrast by 30° arises from different azimuthal angles of the molecules.

To directly resolve these C_{60} orientations, we conducted nc-AFM measurements with a tuning fork sensor at 5 K. Figure 1d shows the frequency shift obtained at constant height z above the second layer of C_{60}, marked 2. Compared to the STM contrast, new intramolecular patterns within C_{60} are resolved by nc-AFM. The contrast of the molecule in the second layer, where relative large positive Δf values of up to ∼40 Hz were measured, clearly indicates different molecular orientations relative to neighboring molecules. Since mainly the long-range vdW forces acting between the tip and the sample above this first C_{60} layer (marked 1 in Figure 1d), the vdW background can be estimated to be roughly −50 Hz. Therefore, the effective Δf due to the short-range interaction forces allowing the submolecular resolution above layer 2 is approximatively 90 Hz. The corresponding force gradient time-averaged over one oscillation cycle with an amplitude of 50 pm is $F' \approx -12.5$ N/m and can be related to a global stiffness probed by the tip above this layer. This large negative force gradient indicates also that the contribution of repulsive Pauli interactions yields to the intramolecular contrast.[19−21] A detailed measurement of the contrast above a molecule is visualized in the narrow scan image in Figure 1e. Inner structures seem to appear on top of the molecule revealing orientation informations. In the image the contrast is composed of polygons with a positive frequency shift ($\Delta f = 100$ Hz)

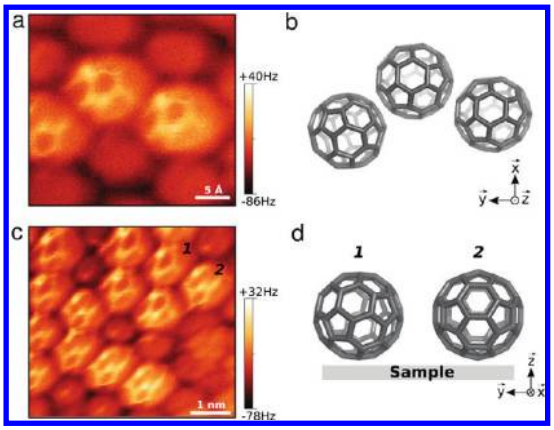

Figure 2. (a) Constant-current nc-AFM image revealing the upper atoms of three C_{60} adsorbed on top of a molecular island (I_t = 58 pA, V_t = +6 mV, oscillation amplitude A = 60 pm). (b) A proposed model of their self-assembly. (c) Constant-current nc-AFM image on a larger area. Two distinct adsorption configurations marked as 1 and 2 can be seen. (d) Model of the adsorption configurations.

and edges appearing slightly darker. The contrast of a carbon ring arises from its center, so-called hollow site, with a more repulsive interaction force compared to its edges. Considering that the tip is terminated by a Cu atom with an atomic radius of 135 pm, this local maxima of the repulsive interaction at the hollow site is induced by the summation of the C−Cu interactions from each atom of the carbon ring.[23,32] Moreover, due to the curvature of the molecule, the Δf of each peripheral surrounding polygon has also a gentle gradient depending on the actual tip−sample distance. The neighboring penta- and hexagonal rings give thus a non-neglectable contribution in the force field and appear as facets (Figure 1e). The sum of all these contributions enhances the visualization of the chemical structure and reveals the C_{60} orientation. Since the achievement of such resolution requires to probe the short-range force regime and owing to a spherical structure, constant height measurements within C_{60} remain challenging and result sometimes in manipulation rather than intramolecular imaging.[33,34] Whereas C_{60} molecules are known to self-assemble with a relative weak binding energy, our measurements show that the closed packed structure of the molecule in multilayers on the Cu(111) substrate can stabilize the system enough to reach the repulsive force region.

To resolve the peripheral structure in a safer way, the actual tip−molecule distance should be kept constant. Figure 2 shows Δf images measured while the tip−sample distance is controlled by keeping a constant tunnelling current (see Supporting Informations Figures S1 and S2). It is true that the STM feedback above a C_{60} induces a variation of the tip−sample distance (∼50 pm) which might have an influence on the nc-AFM images; however, we have shown that the submolecular resolution of AFM can also be achieved in constant height mode as well, which demonstrates the robustness of the method. Contrary to Figure 1d,e, the peripheral rings are clearly resolved. With regards to the positive frequency shift (30 Hz), the imaging conditions are gentle compare to the constant height measurements, and the observed hexagonal patterns again arise due the upper carbon atoms of the molecule. The length of the hexagon edges is estimated to be 1.4 Å, in good agreement with the C−C bond length in a C_{60}.[35] We can also see that, although the tip probes the short-range regime above the adsorbed molecules, the ones involved in the monolayer below could not be atomically resolved. The frequency shift signal recorded above this area is dominated by attractive interaction forces (*ca.* −50 Hz) and thus results in long-range tip−molecule interactions.

The accurate observation of the upper structure within the C_{60} molecules allows an unambiguous understanding of their orientations within molecular islands. A possible lateral arrangement between the molecules, illustrated in the model Figure 2b, can be deduced directly from the experimental data Figure 2a. The Δf map (Figure 2c) presents similar atomic resolution on several self-assembled molecules at a larger scale, and enables also the identification of two different orientations when adsorbed on top of C_{60} islands (marked as 1 and 2 on the figure). The observation of these orientations gives also detailed insights about the molecular interaction with the underlayer since C_{60} has a high degree of symmetry. As illustrated in Figure 2d, molecules in orientation 1 are adsorbed on a benzene ring, and molecules in orientation 2 are absorbed on an edge between adjacent polygons. According to this model, interactions between adjacent molecules among a monolayer arise through edges for the molecule with the relative orientation 1, and through edges and pentagons for the molecule with the relative orientation 2 (Figure 2d).

To further understand the observed contrasts, we carried out systematic three-dimensional spectroscopic measurements at 77 K on different single molecules being adsorbed on top of self-assembled islands. Figure 3 illustrates the evolution of $F_z(x,y)$ and $I_t(x,y)$ at different tip/molecule heights (Figure 3 panels a and b, respectively) as well as vertical cross sections $F_z(x,z)$ and $I_t(x,z)$ (Figure 3c,d, taken along AA′ axis in Figure 3b). For tip−sample distances smaller than 300 pm, the detected contrast in the force field above the molecule, which appears as a homogeneous dark protrusion, is induced by attractive forces of *ca.* −70 pN (z = 250 pm, Figure 3a and region II Figure 3c). In the corresponding I_t map and cross-section, small currents of 10−20 pA are simultaneously recorded. With decreasing tip−sample distance, the I_t intensity becomes larger up to an absolute value of 150−160 pA (z = 0 pm, Figure 3b). The spatial electronic density of states remains without drastic modifications during the tip

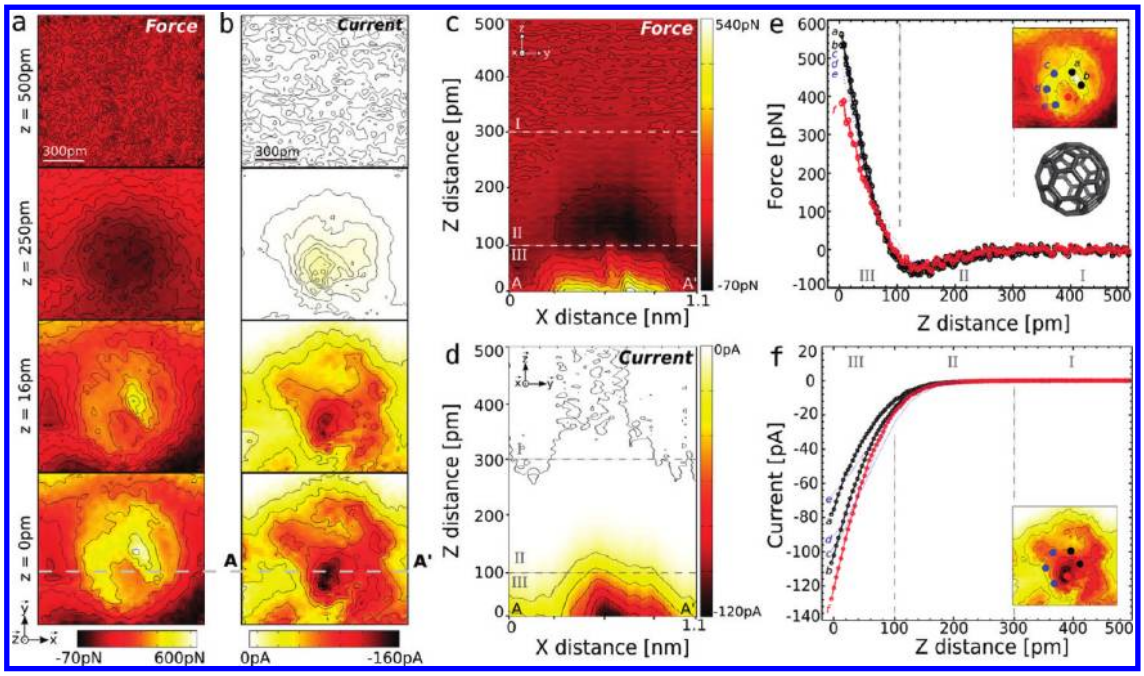

Figure 3. (a, b) Sectional maps of the extracted total force $F_z(x,y)$ and $I_t(x,y)$ measured at different tip−sample distances. (c,d) Vertical cross sections of the $F_z(x,z)$ and $I_t(x,z)$ along the AA' axis shown in panel b. (e, f) Analysis of individual $F_z(z)$ and $I_t(z)$ curves above specific sites described in the insets (V_t = −5 mV, A = 35 pm).

approach and is in good agreement with previous numerical calculations done at the Fermi level.[13] For tip−sample distances smaller than z = 100 pm (region III, Figure 3c), the observed contrast in the F_z map shows first a local decrease at the center of the dark protrusion which even became positive for smaller tip−sample distances (z = 20 pm, Figure 3a). At the closest distance probed during this measurement, the total vertical force is mainly positive above the molecule. The F_z sectional map Figure 3a presents a diagonal bright region at the center of the molecule and contrasts drastically from the one observed in the simultaneous I_t map. In this regime, the tip is mainly influenced by Pauli repulsive forces coming from the upper carbon atoms of the molecule.[19] The observed contrast is thus induced by a C−C bond on top of the molecule similar to orientation 2 described in Figure 2d. Systematic spectroscopic measurements on different molecular sites have been done revealing also the orientation with a top pentagon which corresponds to configuration 1 (see Supporting Informations Figure S3) but we cannot exclude the possibility to find also other orientations.

The analysis of individual force and tunnelling current spectroscopic curves is shown in Figure 3e,f. We focused our interest on specific sites (see inset of Figure 3e) corresponding to carbon sites (marked *a*−*e*) and the center of a carbon ring (*f*). For z distances of the region I and II, the curves are nearly indistinguishable as expected for long-range attractive forces. When the tip−sample distance is smaller than 100 pm within the molecule, we observe strong differences induced by the repulsive force regime. The total interaction force obtained on the upper carbon atoms of the C_{60} (*a* and *b*) attains a maximal value of 550−570 pN. Since the tip−sample distance is larger by a few picometers on similar carbon sites *c*, *d*, and *e* due to the molecular structure, this value is found to be lowered to 460−500 pN. The last curve was obtained at the center of the carbon ring (site *f* of Figure 3c) and as expected exhibits the smallest repulsive force (390 pN). In contrast, the I_t curves simultaneously recorded on the same typical sites (Figure 3f) show different behaviors. The site *f* at the center of the carbon ring has now the highest value of tunnelling current (−130 pA), whereas the different C sites appear with less intensity. According to the small tip−sample voltage used (V_{tip} = −5 mV), the tunnelling current might not reflect directly atomic features but only the local density of states at the Fermi level.

The slopes of the $F(z)$ curves in the repulsive force regime (Figure 3e) correspond to the local force gradient, which can be interpreted as local elastic properties appearing between the structure of the C_{60} molecule and a Cu-terminated tip. Above carbon atoms (black dots *a* and *b* and blue dots *c*−*e*), this vertical force gradient is found to be *ca.* −9 N/m and *ca.* −7 N/m, respectively, whereas above the center of the carbon ring (red dot *f*) this value is lowered to *ca.* −4 N/m. Therefore it reveals that different site-dependent stiffnesses exist between the molecular structure and the tip. Since the dissipation signal was extremely small (≤10 meV/cycle), we conclude that the deformations are purely elastic and that plastic

deformations can be neglected. Indeed, the linear behavior of the $F(z)$ curves observed in the repulsive force regime confirms these elastic deformations and also shows the requirement of a stable tip−molecule junction. Since a softer tip compared to the molecule would not give intramolecular resolutions as shown in Figure 3a, we believe that the observed site-dependent force variations are related to local stiffness variations of the C_{60} structure.

The tip−sample interaction potential U were then calculated by integrating F_z along the z direction. Thereafter, we extracted the lateral force F_x by differentiation of U along the x direction. The maximum F_x in the repulsive regime is *ca.* 10−15 pN, whereas in the attractive regime this value is almost zero (≤ -2 pN). The corresponding lateral force gradient is thus *ca.* −0.1−0.2 N/m. Considering that in our measurement the tip trajectory is always vertical and the detected lateral forces extremely small,[36] we can conclude that the C_{60} molecule is not rotated. The controlled manipulation of this molecule would be more efficient by laterally pushing the side of the cage structure rather than pressing at the top.[33,34,37]

CONCLUSION

In summary, these results demonstrate a systematic observation of the C_{60} orientations on Cu(111) by achieving intramolecular resolution by nc-AFM. Three-dimensional force field spectroscopy shows that no C_{60} manipulation is induced during measurements and characterizes the tip−sample interaction forces, coming from Pauli repulsive forces, required to reach such resolutions. Moreover, atomic-scale tip−sample stiffnesses are detected above the cage structure which are related to local stiffness variations of the C_{60} structure. We anticipate that such parallel studies of the atomic structure and the local electronic density of states of molecules will yield detailed insights about intermolecular interactions in self-assembled systems and functional groups involved in chemical reaction on surfaces, and will also give systematic informations about the intrinsic elastic properties of single molecules at the atomic scale.

EXPERIMENTAL SECTION

Sample Preparation. The Cu(111) substrate was prepared into the vacuum chamber with a base pressure lower than 5×10^{-10} mbar by repeated Ar^+ sputtering and subsequent annealing cycles (870 K). The C_{60} molecules were then thermally evaporated from a quartz glass crucible heated up to 620 K onto the substrate being kept at room temperature. The deposition rate was determined with a quartz microbalance and from large-scale STM images at ∼0.5 ML/min in these conditions.

STM/nc-AFM Experiments. STM and nc-AFM experiments were performed with a commercial qPlus STM/AFM microscope (Omicron Nanotechnology GmbH) running at low temperature (77 and 5 K) under ultrahigh vacuum lower than 1×10^{-10} mbar and operated by a Nanonis Control Systems from SPECS GmbH. We used a commercial tuning-fork sensor (resonance frequency $f_0 \approx 26$ kHz, spring constant $k_0 \approx 1800$ N/m, typical quality factor $Q = 11\,000$ at 77 K, $Q = 20000-60000$ at 5 K). All STM images were recorded at constant current mode with the bias voltage applied to the tip. The nc-AFM images were performed at constant height or at constant current (see Supporting Information Figure S1 and Figure S2). During nc-AFM experiments, low bias voltage was always applied in order to minimize the tunnelling current flow and prevent a possible disturbance of the modulation of electrostatic forces at the tip apex in the Δf signal. Oscillation amplitudes of the tuning fork were always set below 100 pm. Since the tip was indented several times to the substrate before measurements to improve its quality, we assume that the apex was functionalized with copper adatoms.

Three-Dimensional Spectroscopic Measurements. During spectroscopic measurements, the frequency shift $\Delta f(z)$ and the tunnelling current $I_t(z)$ *versus* distance z curves were recorded simultaneously above single molecules at 77 K in order to construct a box of 1.2 nm × 1.2 nm × 0.5 nm length containing 61 × 60 × 128 data points. During measurement, the thermal drift was compensated by using atom-tracked positioning[38] before each z distance measurement. Additionally, a $\Delta f(z)$ curve was taken (typical sweep distance *ca.* 5−10 nm) after the complete measurement. Thereafter, the total vertical force F_z was extracted from the collected data utilizing the Sader and Jarvis formula.[39]

Acknowledgment. We acknowledge financial support from the Swiss National Science Foundation (SNF), the ESF EUROCORE program FANAS, and the Swiss National Center of Competence in Research on "Nanoscale Science" (NCCR-NANO).

Supporting Information Available: Illustration of the two different data acquisition modes used for nc-AFM imaging above a single C_{60}; combined STM/nc-AFM measurement revealing the different molecular contrasts; additional 3D-spectroscopic measurements of $F_z(z)$ and $I_t(z)$ describing the molecular orientation with a top pentagon. This material is available free of charge *via* the Internet at http://pubs.acs.org.

REFERENCES AND NOTES

1. Kroto, H. W.; Heath, J. R.; O'Brien, S. C.; Curl, R. F.; Smalley, R. E. C_{60}: Buckminsterfullerene. *Nature* **1985**, *318*, 162–163.
2. Hebard, A. F.; Rosseinsky, M. J.; Haddon, R. C.; Murphy, D. W.; Glarum, S. H.; Palstra, T. T. M.; Ramirez, A. P.; Kortan, A. R. Superconductivity at 18 K in Potassium-Doped C_{60}. *Nature* **1991**, *350*, 600–601.
3. Park, H.; Park, J.; Lim, A. K. L.; Anderson, E. H.; Alivisatos, A. P.; McEuen, P. L. Nanomechanical Oscillations in a Single-C_{60} Transistor. *Nature* **2000**, *407*, 57–60.
4. Winkelmann, C. B.; Roch, N.; Wernsdofer, W.; Bouchiat, V.; Balestro, F. Superconductivity in a Single-C_{60} Transistor. *Nat. Phys.* **2009**, *5*, 876–879.
5. Schull, G.; Frederiksen, T.; Arnau, A.; Sànchez-Portal, D.; Berndt, R. Atomic-Scale Engineering of Electrodes for Single-Molecule Contacts. *Nat. Nanotechnol.* **2010**, *6*, 23–27.
6. Néel, N.; Kröger, J.; Limot, L.; Berndt, R. Conductance of Oriented C_{60} Molecules. *Nano Lett.* **2008**, *8*, 1291–1295.
7. Schull, G.; Frederiksen, T.; Brandbyge, M.; Berndt, R. Passing Current through Touching Molecule. *Phys. Rev. Lett.* **2009**, *103*, 206803-1–206803-4.
8. Binnig, G.; Rohrer, H.; Gerber, Ch.; Weibel, E. Surface Studies by Scanning Tunnelling Microscopy. *Phys. Rev. Lett.* **1982**, *49*, 57–61.
9. Barth, J. V. Molecular Architectonic on Metal Surfaces. *Annu. Rev. Phys. Chem.* **2007**, *58*, 375–407.
10. Gourdon, A. On-Surface Covalent Coupling in Ultrahigh Vacuum. *Angew. Chem., Int. Ed.* **2008**, *47*, 6950–6953.
11. Zwaneveld, N. A. A.; Pawlak, R.; Abel, M.; Catalin, D.; Gigmes, D.; Bertin, D.; Porte, P. Organized Formation of

2D-Extended Covalent Organic Frameworks at Surfaces *J. Am. Chem. Soc.* **2008**, *130*, 6678–6679.
12. Lu, X.; Grobis, M.; Khoo, K. H.; Louie, S. G.; Crommie, M. F. Spatially Mapping the Spectral Density of a Single C_{60} Molecule. *Phys. Rev. Lett.* **2030**, *90*, 096802-1–096802-4.
13. Hashizume, T.; Motai, K.; Wang, X. D.; Shinohara, H.; Saito, Y.; Maruyama, Y.; Ohno, K.; Kawazoe, Y.; Nishina, Y.; Pickering, H. W.; *et al*. Intramolecular Structures of C_{60} Molecules Adsorbed on the Cu(111)-(1 × 1) Surface. *Phys. Rev. Lett.* **1993**, *71*, 2959–2962.
14. Larsson, J. A.; Elliott, S. D.; Greer, J. C.; Repp, J.; Meyer, G.; Allenspach, R. Orientation of individual C_{60} Molecules Adsorbed on Cu(111): Low-Temperature Scanning Tunnelling Microscopy and Density Functional Calculations. *Phys. Rev. B* **2008**, *777*, 115434-1–115434-9.
15. Schull, G.; Berndt, R. Orientationally Ordered (7 × 7) Superstructure of C_{60} on Au(111). *Phys. Rev. Lett.* **2007**, *99*, 226105-1–226105-4.
16. Giessibl, F. J. Atomic Resolution of the Silicon (111)-(7 × 7) Surface by Atomic Force Microscopy. *Science* **1995**, *267*, 68–71.
17. Morita, S., Wiesendanger, R., Meyer, E., Eds. Noncontact Atomic Force Microscopy. In *NanoScience and Technology*; Springer: New York, 2002.
18. Meyer, E.; Glatzel, T. Novel Probes for Molecular Electronics. *Science* **2009**, *324*, 1397–1398.
19. Gross, L.; Mohn, F.; Moll, N.; Liljeroth, P.; Meyer, G. The Chemical Structure of a Molecule Resolved by Atomic Force Microscopy. *Science* **2009**, *325*, 1110–1114.
20. Gross, L.; Mohn, F.; Moll, N.; Meyer, G.; Ebel, R.; Abdel-Mageed, W. M.; Jaspars, M. Organic Structure Determination Using Atomic-Resolution Scanning Probe Microscopy. *Nat. Chem.* **2010**, *2*, 821–825.
21. Mohn, F.; Repp, J.; Gross, L.; Meyer, G.; Dyer, M. S.; Persson, M. Reversible Bond Formation in a Gold-Atom Organic-Molecule Complex as a Molecular Switch. *Phys. Rev. Lett.* **2010**, *105*, 266102-1–266102-14.
22. Allers, W.; Schwarz, A.; Schwarz, U. D.; Wiesendanger, R. Dynamic Scanning Force Microscopy at Low Temperature on a van der Waals Surface: Graphite (0001). *Appl. Surf. Sci.* **1999**, *140*, 247–252.
23. Hembacher, S.; Giessibl, F. J.; Mannhart, J. Force Microscopy with Light-Atom Probes. *Science* **2004**, *305*, 380–383.
24. Albers, B. J.; Schwendemann, T. C.; Baykara, M. Z.; Pilet, N.; Liebmann, M.; Altman, E. I.; Schwarz, U. D. Three-Dimensional Imaging of Short-Range Chemical Forces with Picometre Resolution. *Nat. Nanotechnol.* **2009**, *4*, 307–310.
25. Kawai, S.; Kawakatsu, H. Surface-Relaxation-Induced Giant Corrugation on Graphite (0001). *Phys. Rev. B* **2009**, *79*, 115440-1–115440-5.
26. Kawai, S.; Glatzel, T.; Koch, S.; Such, B.; Baratoff, A.; Meyer, E. Ultrasensitive Detection of Lateral Atomic-Scale Interactions on Graphite (0001) *via* Bimodal Dynamic Force Measurements. *Phys. Rev. B* **2010**, *81*, 085420-1–085420-7.
27. Ashino, M.; Schwarz, A.; Behnke, T.; Wiesendanger, R. Atomic-Resolution Dynamic Force Microscopy and Spectroscopy of a Single-Walled Carbon Nanotube: Characterization of Interatomic van der Waals Forces. *Phys. Rev. Lett.* **2004**, *93*, 136101-1–136101-4.
28. Ashino, M.; Obergfell, D.; Haluska, M.; Yang, S.; Khlobystov, A. N.; Roth, S.; Wiesendanger, R. Atomically Resolved Mechanical Response of Individual Metallofullerene Molecules Confined Inside Carbon Nanotubes. *Nat. Nanotechnol.* **2008**, *3*, 337–341.
29. Burke, S. A.; Mativetsky, J. M.; Hoffmann, R.; Grütter, P. Nucleation and Submonolayer Growth of C_{60} on KBr. *Phys. Rev. Lett.* **2005**, *94*, 096102-1–096102-4.
30. Burke, S. A.; Mativetsky, J. M.; Fostner, S.; Grütter, P. C_{60} on Alkali Halides: Epitaxy and Morphology Studied by Noncontact AFM. *Phys. Rev. B* **2007**, *76*, 035419-1–035419-9.
31. Zerweck, U.; Loppacher, Ch.; Otto, T.; Grafström, S.; Eng, L. M. Kelvin Probe Force Microscopy of C_{60} on Metal Substrates: Towards Molecular Resolution. *Nanotechnology* **2007**, *18*, 084003-1–084003-5.
32. Ondráček, M.; Pou, P.; Rozsval, V.; González, C.; Jelnek, P.; Pérez, R. Forces and Currents in Carbon Nanostructures: Are We Imaging Atoms?. *Phys. Rev. Lett.* **2011**, *106*, 176101-1–176101-4.
33. Keeling, D. L.; Humphry, M. J.; Fawcett, R. H. J.; Beton, P. H.; Hobbs, C.; Kantorovich, L. Bond Breaking Coupled with Translation in Rolling of Covalently Bound Molecules. *Phys. Rev. Lett.* **2005**, *94*, 146104–1/4.
34. Martsinovich, N.; Hobbs, C.; Kantorovich, L.; Fawcett, R. H. J.; Humphry, M. J.; Keeling, D. L.; Beton, P. H. C_{60} Adsorption on the Si(111)-p(7 × 7) Surface: A Theoretical Study. *Phys. Rev. B* **2006**, *94*, 085304-1–085304-12.
35. Yannoni, C. S.; Bernier, P. P.; Bethune, D. S.; Meijer, G.; Salem, J. R. NMR Determination of the Bond Lengths in C_{60}. *J. Am. Chem. Soc.* **1991**, *113*, 3190–3192.
36. Ternes, M.; Lutz, C. P.; Hirjibehedin, C. F.; Giessibl, F. J. The Force Needed To Move an Adatom on a Surface. *Science* **2008**, *319*, 1066–1069.
37. Cuberes, M. T.; Schlittler, R. R.; Gimzewski, J. K. Repositioning of C_{60} Molecules on Surfaces at Room Temperature. *App. Phys. Lett.* **1996**, *69*, 3016–3019.
38. Kawai, S.; Glatzel, T.; Koch, S.; Baratoff, A.; Meyer, E. Interaction-Induced Atomic Displacements Revealed by Drift-Corrected Dynamic Force Spectroscopy. *Phys. Rev. B* **2011**, *83*, 035421-1–035421-7.
39. Sader, J. E.; Jarvis, S. P. Accurate Formulas for Interaction Forces and Energy in Frequency Modulation Force Spectroscopy. *App. Phys. Lett.* **2004**, *84*, 1801–1803.